Projected atomic orbitals as optimal virtual space for excited state projection-based embedding calculations

Ádám B. Szirmai,[†,‡] Bence Hégely,[¶,§,‖] Attila Tajti,[*,†] Mihály Kállay,[¶,§,‖] and Péter G. Szalay[*,†]

†*Laboratory of Theoretical Chemistry, Institute of Chemistry, ELTE Eötvös Loránd University, P. O. Box 32, H-1518, Budapest 112, Hungary*

‡*György Hevesy Doctoral School, ELTE Eötvös Loránd University, Institute of Chemistry*

¶*Department of Physical Chemistry and Materials Science, Faculty of Chemical Technology and Biotechnology, Budapest University of Technology and Economics, Műegyetem rkp. 3., H-1111 Budapest, Hungary*

§*ELKH-BME Quantum Chemistry Research Group, Műegyetem rkp. 3., H-1111 Budapest, Hungary*

‖*MTA-BME Lendület Quantum Chemistry Research Group, Műegyetem rkp. 3., H-1111 Budapest, Hungary*

E-mail: attila.tajti@ttk.elte.hu; szalay@chem.elte.hu

Abstract

The projected atomic orbitals (PAO) technique is presented for the construction of virtual orbital spaces in projection-based embedding (PbE) applications. The proposed straightforward procedure produces a set of virtual orbitals, which is used in

the final, high-level calculation of the embedded active subsystem. The PAO scheme is demonstrated on intermolecular potentials of bimolecular complexes, in ground and excited states, including Rydberg excitations. The results show the outstanding performance of the PbE method when used with PAO virtual orbitals compared to those produced using common orbital localization techniques. The good agreement of the resulting PbE potential curves with those from high-level *ab initio* dimer calculations, also in diffuse basis sets, confirms that the PAO technique can be suggested for future applications using top-down embedding methods.

Keywords: excited states, intermolecular interactions, embedding, PAOs

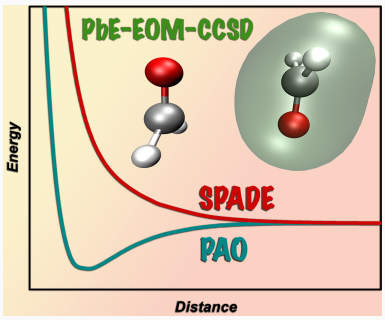

Embedding techniques[1] have emerged to be some of the most effective approaches to overcome the serious limitations of the applicability of high-level quantum chemistry methods due to the system size. This family of methods treat the relevant subsystem (reaction center, chromophore, etc.) at a higher level of theory while including the effect of the other parts in an approximate way, e.g., by using lower-level methods. Density Functional Theory (DFT) methods are ideal for embedding applications provided that the density can be distributed between the fragments and the functional form of the interactions allows a suitable definition of the embedding potential. Wave-function-in-DFT (WF-in-DFT) embedding[2,3] approaches allow the treatment of the active fragment by advanced *ab initio* techniques, while the environment is modeled at the DFT level. In particular, various formulations of Coupled Cluster theory[4–7] are commonly invoked for the active subsystem(s) also in excited electronic states,[8–14] where the accuracy of these methods is often warranted even for a qualitatively correct description. Two major types of these embedding techniques are the so-called bottom-up (frozen density)[2,3] and the top-down[4,5] approaches. The problematic point of the former is the calculation of some non-additive terms.[15] These are avoided in top-down projector-based embedding techniques which maintain the orthogonality of the subsystems by applying appropriate projectors, however, a low-level calculation on the entire system is necessary. While for non-covalently interacting systems the non-additive terms are less crucial, for higher accuracy and for generalizability top-down projection-based embedding (PbE)[4] methods seem more suited for the description of multichromophore systems.[16]

In the top-down models a low-level calculation (usually at the DFT level) is performed first on the entire system, followed by a localization of the occupied orbitals on *a priori* defined sets of atoms (subsystems). This latter step is usually accomplished by using Pipek–Mezey localization,[17] intrinsic bond orbitals,[18] or the SPADE (Subsystem Projected AO DEcomposition)[19] technique and the orbital space belonging to the different fragments, which is then used to set up the embedding potential from the fragments' density, is defined by the position of the resulting localized orbitals. Subsequently, the orbitals of the active subsystem(s) are reoptimized under the influence of the embedding potential, applying the orthogonality constrain between the subsystems by level shifting,[4] solving the Huzinaga equation,[5] or by applying the projection scheme by Hoffmann et al.[20] The high-level correlated calculations

on the active fragment are finally performed using the Fock matrix that results from the above procedure. Since only the electrons defining the density on the active fragment(s) are used in these calculations, a significant reduction of the cost of the calculation is achieved. Details of the PbE workflow used in this study are described in Section S1.3 (see also Refs. 12 and 16).

Nevertheless, the original formulations of PbE[4,5] leave the space of virtual orbitals intact, i.e., that of the original supersystem, which poses serious limitations on the applicability of the higher-level *ab initio* methods due to the unfavorable scaling of the computational cost with the size of the virtual space.[21] In addition, the untruncated virtual space tendentially leads to the appearance of artefactual low-lying charge transfer (CT) states,[16] often rendering the identification of local excited states impossible. Several approaches have been investigated to deal with this problem by truncating the virtual space in a reasonable way, including the absolutely localized embedding schemes of Chulhai and Goodpaster[6,9] that avoid the issue entirely by using monomer basis sets, or the basis set truncation method for PbE by Bennie et al.[22] which relies on net Mulliken population criteria. Claudino and Mayhall developed a concentric virtual orbital localization technique[21] which uses a (smaller) projection basis to assign a virtual subspace to atoms and then span the virtual space by iteratively including more and more virtual orbitals belonging also to the environment. This technique has been used by Parravicini and Jagau in embedded excited state calculations.[11] Visscher and co-workers generalized the intrinsic atomic orbital approach[18] to molecular fragments,[23] constructing orthogonal localized orbitals by spanning the supersystem valence and virtual space[24] using reference fragment orbitals. Conventional MO-based localization, such as Pipek–Mezey[17] and SPADE[19] can also be applied to the virtual space, and by assigning orbitals to the subsystems based on some selection criteria, those of the environment can be discarded.[25] Using the original SPADE algorithm[19] for the virtual orbitals we observed,[16] however, that without any further adjustments the resulting virtual space can be severely distorted compared to that of an isolated monomer. As suggested in Ref. 16, the distortion can be reduced by extending the space by some environment orbitals that show the largest overlap with the atomic orbitals centered on the active subsystem (called the "extended SPADE" approach hereafter). Nevertheless, the effective construction of appropriate

virtual orbitals, especially if diffuse basis functions are present, remains a challenge in PbE applications. Improper virtual spaces can cause a drastic overestimation of the energy and result in nonphysically repulsive intermolecular potentials,[16] calling for a compelling remedy for this issue. In this letter, the use of projected atomic orbitals (PAOs) is suggested as an alternative for creating virtual orbitals localized on the active subsystem.

PAOs were first suggested by Boughton and Pulay[26] to define the virtual space in local correlation calculations. We suggest the implementation of this concept in PbE, relying on the use of the atomic orbitals centered on the active subsystem's atoms as the basis for the construction of a virtual space (the PAOs).

We define the projector of the occupied orbitals of the supersystem as

$$\mathbf{R} = \mathbf{C}_{\mathrm{occ}}\mathbf{C}_{\mathrm{occ}}^{\mathrm{T}}, \tag{1}$$

where $\mathbf{C}_{\mathrm{occ}}$ is the occupied orbital block of the MO coefficient matrix. The application of this projector leads to the PAOs

$$\mathbf{C}_{\mathrm{PAO}} = \mathbf{1} - \mathbf{RS}, \tag{2}$$

where $\mathbf{S}$ is the AO overlap matrix. These orbitals are projected into the basis of the active subsystem, similarly to the first step in the concentric localization procedure by Claudino and Mayall.[21] This is done in such a way that the resulting orbitals span the virtual space of the active fragment, which is enforced by a truncation based on the norm of the PAOs, dropping all orbitals that have negligible contribution to the active subsystem's virtual space. The norms are obtained as

$$N_i = \sum_{\mu}^{\mathrm{act.AOs}} (\mathbf{C}_{\mathrm{PAO}})_{i\mu}(\mathbf{SC}_{\mathrm{PAO}})_{i\mu} \ , \tag{3}$$

where the indices μ and i label AOs of the active subsystem (act.AOs) and the PAOs, respectively, and the PAOs with N_i below an appropriately chosen small threshold value are discarded. The remaining orbitals are renormalized, producing a new set of PAOs, $\mathbf{C}'_{\mathrm{PAO}}$.

To eliminate linear dependencies from this set, a second truncation step is introduced by

screening the redundant PAOs via the diagonalization of their overlap matrix

$$\mathbf{S}_{\mathrm{PAO}} = (\mathbf{C}'_{\mathrm{PAO}})^{\mathrm{T}}\, \mathbf{S}\, \mathbf{C}'_{\mathrm{PAO}}, \tag{4}$$

so that only PAOs with an absolute value of their eigenvalue $|s_i|$ above a chosen truncation parameter are retained. The resulting set of linearly independent PAOs are finally used as the virtual orbital basis when solving the Huzinaga equation.[5] Details are given in Section S1.3 of the Supporting Information.

The generation of PAOs using the above scheme thus requires the definition of the atoms used for the construction of the PAOs, as well as two truncation parameters, one for the post-projection norm (N_i) and another for the tolerance of the overlap for redundant orbitals ($|s_i|$). In our experience, the dimension of the resulting virtual space is the same as that of the bare monomer, except at the shortest intermolecular separations. This is very important since this way the cost of the embedded calculation on the active fragment does not exceed that of an isolated monomer. This scheme has been implemented in the MRCC program code.[27,28]

We evaluate the effect of the virtual space truncation on the quality of the interaction potential energy curves, both in ground and excited states, for the stacked homodimers of formaldehyde [$(CH_2O)_2$] and pyrrole [$(Pyr)_2$], as well as for the cytosine-uracil complex [Cyt-Ura]. The structures of the complexes are available in the Supporting Information. The investigated excited states are selected such that, for simplicity, the two-state model is valid for them, except for very short intermolecular distances in certain cases. The same states have been studied in a recent work[16] and the PbE technique using the SPADE-based localization of virtual orbitals was found to give unphysical potential energy surfaces in most cases. As reference, we use Coupled Cluster with Singles and Doubles (CCSD)[29] and Equation-of-Motion Coupled Cluster with Singles and Doubles (EOM-CCSD)[30,31] calculations for the ground and excited states, respectively, corrected for the basis set superposition error (BSSE). The same wave function methods are employed in the WF-in-DFT type PbE, with the low-level DFT calculations using the Perdew–Burke–Ernzerhof (PBE) functional.[32] For the excited states of the homodimers, a single reference curve is obtained by averaging

the energies of the two interacting states, that is, by removing the excitonic coupling. This choice allows the comparison of the calculated curves without any bias arising from the approximation used for the latter quantity. In the case of the [Cyt-Ura] heterodimer this is not possible and in this example the interaction of the two states via excitonic couplings is also included in the embedding models using the scheme described in Ref. 16 (see the Supporting Information for more details and Ref. 16 for discussion on the validity of this approximation). To make meaningful comparisons to the reference, the interaction energy has to be augmented by a dispersion correction,[16,25] for which the D3 dispersion correction by Grimme was chosen.[33] Since in the present scheme the interaction energy is described by DFT, this choice is in accordance with Szalewicz's finding.[34] All calculations have been performed by the MRCC suite of codes.[27,28] Further details of the test calculations can be found in the Supporting Information.

In panel A of Figure 1, the ground state potential energy curves for the $[(CH_2O)_2]$ dimer are shown, calculated with four different virtual spaces: the full virtual space, one localized with the SPADE procedure, the latter extended by two additional virtual orbitals "ext. SPADE"), as well as with the space produced with the PAO scheme. Note that the SPADE and PAO schemes are using the same number of virtual orbitals which is that of the monomer. It is clearly seen that while with the full valence space the interaction energy is slightly overestimated, the SPADE localization results in a far too small interaction energy. Adding the two environment orbitals with the largest overlap with the AOs of the active subsystem improves the results considerably, while with PAO virtual orbitals an almost perfect curve is obtained.

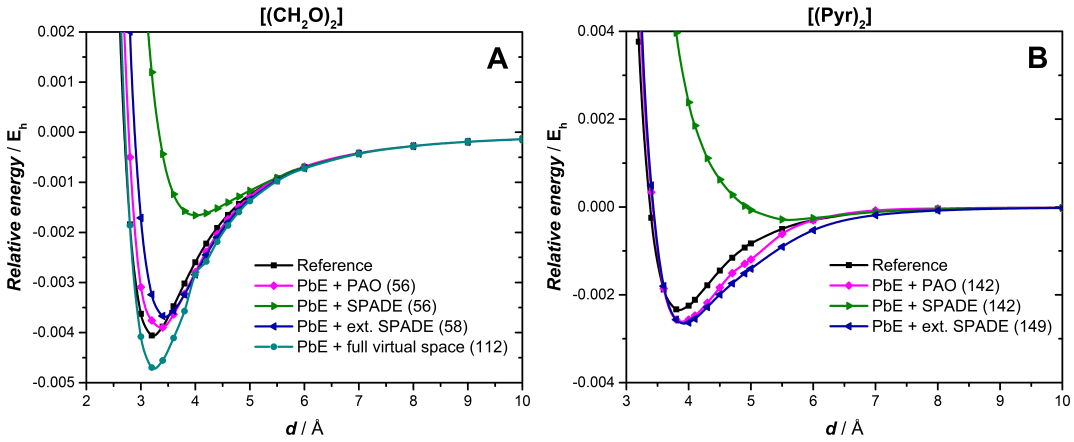

Figure 1: CCSD ground-state interaction energies (in atomic units) of the $[(CH_2O)_2]$ (Panel A, $N = 0.05$, $s = 10^{-3}$) and $[(Pyr)_2]$ (Panel B, $N = 0.05$, $s = 9 \cdot 10^{-5}$) homodimer complexes as functions of the intermolecular separation d, evaluated in the aug-cc-pVDZ basis. In the legend, the numbers in parenthesis give the number of virtual orbitals used in the various calculations at $d = 5$Å.

Similar conclusions can be drawn in the case of $[(Pyr)_2]$ (Panel B of Figure 1), where again the PAO virtual space gives the best potential energy curves. (Note that for this system the "ext. SPADE" variant includes seven additional orbitals.)

For the Rydberg type excited states obtained in the diffuse aug-cc-pVDZ basis (Figure 2), the SPADE localization results in repulsive interaction curves. This is the consequence of, as discussed in Ref. 16, the requirement that for the correct description of the Rydberg states the virtual orbitals have to extend to the space where the other fragment resides. However, the standard localization procedures (e.g. the symmetric orthogonalization of the basis functions in SPADE) cut off this part of the virtual basis, deteriorating the wave function more and more with decreasing distance between the fragments. We have called this effect the *reverse BSSE* in Ref. 16. As evident from Panel A of Figure 2, the extension of the virtual space by the most overlapping orbitals of the environment does not solve the problem, the respective potential curve is still repulsive. On the other hand, the use of a PAO virtual space provides a solution here since the diffuse functions of the active fragments are retained in the basis, irrespective of their overlap with the other fragment. In the case of $[(CH_2O)_2]$ (Panel A), we again get a nearly perfect curve with PAOs, while the improvement is also apparent for the two investigated Rydberg states of $[(Pyr)_2]$ (Panels B and C). Note that in the latter system, at short distances the two-state model is not valid anymore, thus

a good agreement of PbE and the reference is only expected at separations above 4 Å.[16]

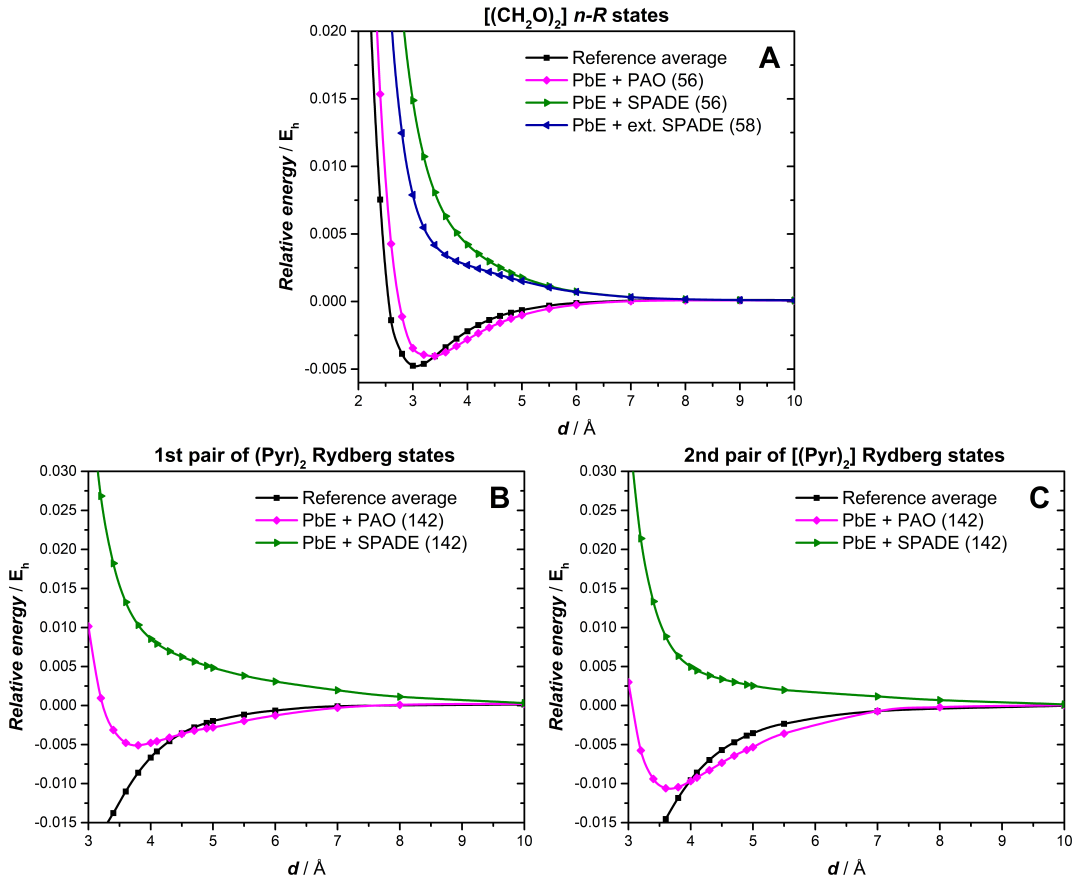

Figure 2: EOM-CCSD averaged interaction energies of different Rydberg excited state pairs in the $[(CH_2O)_2]$ (Panel A, $N = 0.05$, $s = 10^{-3}$) and $[(Pyr)_2]$ (Panels B and C, $N = 0.05$, $s = 9 \cdot 10^{-5}$) homodimer complexes as functions of the intermolecular separation d, evaluated in the aug-cc-pVDZ basis. In the legend, the numbers in parenthesis give the number of virtual orbitals used in the various calculations at $d = 5$Å.

This issue also affects the $\sigma - \pi^*$ and $\pi - \pi^*$ valence excited states of $[(CH_2O)_2]$ calculated in the aug-cc-pVDZ basis, shown on panels A and B of Figure 3. Nevertheless, only the curves obtained with PAO virtual orbitals are attractive, fixing the qualitatively wrong repulsive behavior of the ones based on the SPADE localization. Since here the breakdown of the two-state model affects the reference curves more strongly,[16] their agreement with PbE is less good than in the examples above.

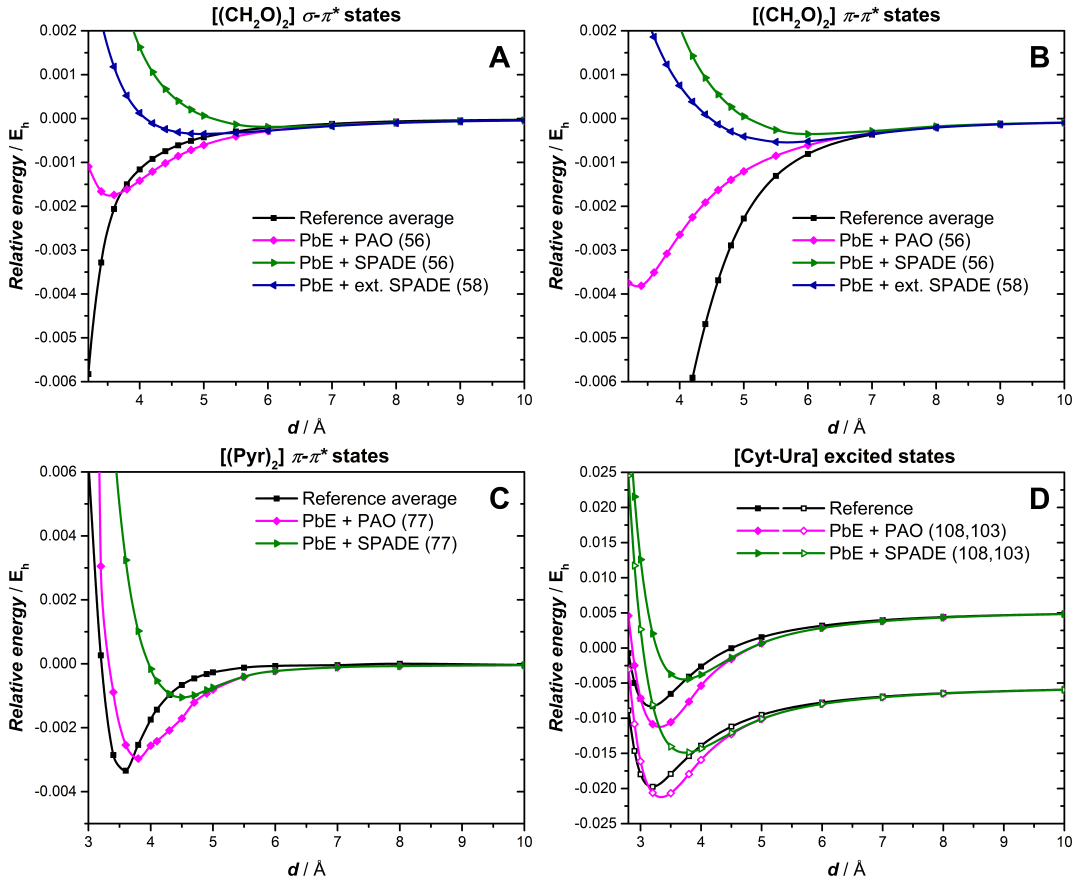

Figure 3: EOM-CCSD averaged interaction energies of different valence excited state pairs: $\sigma - \pi^*$ and $\pi - \pi^*$ states of the $[(CH_2O)_2]$ complex (Panels A and B, aug-cc-pVDZ basis, $N = 0.05$, $s = 10^{-3}$) and $\pi - \pi^*$ excited states of the $[(Pyr)_2]$ homodimer complex (Panel C, cc-pVDZ basis, $N = 0.05$, $s = 10^{-3}$), and the $\pi - \pi^*$ excited states of the [Cyt-Ura] complex (Panel D, no averaging, cc-pVDZ basis, $N = 0.05$, $s = 10^{-3}$) as functions of the intermolecular separation d. In the legend, the numbers in parenthesis give the number of virtual orbitals used in the various calculations at $d = 5$Å. In the case of [Cyt-Ura], the two numbers refer to the cytosine and uracil calculations, respectively.

The validity of the two-state model is often broader if the basis set does not include diffuse functions since Rydberg and Charge Transfer (CT) states are pushed to higher energies. This choice makes the study of the valence excited states possible with the disadvantage of less accurate interaction energies. In panel C of Figure 3, the curves obtained for the π-π^* state of $[(Pyr)_2]$ with the cc-pVDZ basis set are shown, and the PAO technique is indeed found to perform excellently in this non-diffuse basis. Note, however, that the truncation based on the SPADE localization also gives an attractive, although less accurate potential curve for this state. This proper behavior can be explained by the small overlap of the active fragment

orbitals with the environment, even at short distances.

Also for the pair of $\pi - \pi^*$ excited states of the [Cyt-Ura] complex shown in Panel D of Figure 3, the SPADE method predicts bound configurations, but the interaction energy and the equilibrium distance are significantly under- and overestimated, respectively. Compared to these curves, the PAO approach brings a clear improvement yet again and a satisfactory agreement with the reference calculations.

In summary, the results presented here show the superior performance of the PAOs for virtual orbital space with the PbE embedding method. Not only are the calculations cheap (the same as the calculation on the bare fragment), but the potential curves follow the reference curves obtained for the supersystem nicely. This is true for both ground and excited states, including both valence and Rydberg type excitations. Since the problem of virtual space truncation, which is solved effectively by the presented approach, affects any top-down embedding strategy that relies on orbital localization, we advocate the use of a PAO virtual space in all such applications, especially those employing diffuse basis sets.

Acknowledgments

This work has been supported by the National Research, Innovation and Development Fund (NKFIA) of Hungary Grant No. 142634 and KKP126451. The authors thank Bónis Barcza for discussions.

Data availability statement

The data supporting the findings of this study are available in the supplementary material.

Conflict of interest

The authors declare no conflict of interest.

Supporting Information

Details of the calculations, structures of the monomers and complexes evaluated in this study.

References

1. Goez, A.; Neugebauer, J. In *Frontiers of Quantum Chemistry*; Wójcik, M. J., Nakatsuji, H., Kirtman, B., Ozaki, Y., Eds.; Springer Singapore: Singapore, 2018; pp 139–179.

2. Govind, N.; Wang, Y.; da Silva, A.; Carter, E. Accurate ab initio energetics of extended systems via explicit correlation embedded in a density functional environment. *Chemical Physics Letters* **1998**, *295*, 129–134.

3. Wesołowski, T. A. Embedding a multideterminantal wave function in an orbital-free environment. *Physical Review A* **2008**, *77*, 012504.

4. Manby, F. R.; Stella, M.; Goodpaster, J. D.; Miller, T. F. I. A Simple, Exact Density-Functional-Theory Embedding Scheme. *Journal of Chemical Theory and Computation* **2012**, *8*, 2564–2568, PMID: 22904692.

5. Hégely, B.; Nagy, P. R.; Ferenczy, G. G.; Kállay, M. Exact density functional and wave function embedding schemes based on orbital localization. *The Journal of Chemical Physics* **2016**, *145*, 064107.

6. Chulhai, D. V.; Goodpaster, J. D. Improved Accuracy and Efficiency in Quantum Embedding through Absolute Localization. *Journal of Chemical Theory and Computation* **2017**, *13*, 1503–1508.

7. Höfener, S.; Severo Pereira Gomes, A.; Visscher, L. Molecular properties via a subsystem density functional theory formulation: A common framework for electronic embedding. *The Journal of Chemical Physics* **2012**, *136*, 044104.

8. Bennie, S. J.; Curchod, B. F. E.; Manby, F. R.; Glowacki, D. R. Pushing the Limits of EOM-CCSD with Projector-Based Embedding for Excitation Energies. *The Journal of Physical Chemistry Letters* **2017**, *8*, 5559–5565, PMID: 29076727.

9. Wen, X.; Graham, D. S.; Chulhai, D. V.; Goodpaster, J. D. Absolutely Localized Projection-Based Embedding for Excited States. *Journal of Chemical Theory and Computation* **2020**, *16*, 385–398, PMID: 31769981.

10. Zech, A.; Ricardi, N.; Prager, S.; Dreuw, A.; Wesolowski, T. A. Benchmark of Excitation Energy Shifts from Frozen-Density Embedding Theory: Introduction of a Density-Overlap-Based Applicability Threshold. *Journal of Chemical Theory and Computation* **2018**, *14*, 4028–4040, PMID: 29906111.

11. Parravicini, V.; Jagau, T.-C. Embedded equation-of-motion coupled-cluster theory for electronic excitation, ionisation, electron attachment, and electronic resonances. *Molecular Physics* **2021**, *119*, e1943029.

12. Hégely, B.; Szirmai, Á. B.; Mester, D.; Tajti, A.; Szalay, P. G.; Kállay, M. Performance of Multilevel Methods for Excited States. *The Journal of Physical Chemistry A* **2022**, *126*, 6548–6557, PMID: 36095318.

13. Gomes, A. S. P.; Jacob, C. R.; Visscher, L. Calculation of local excitations in large systems by embedding wave-function theory in density-functional theory. *Physical Chemistry Chemical Physics* **2008**, *10*, 5353–5362.

14. Höfener, S.; Gomes, A. S. P.; Visscher, L. Solvatochromic shifts from coupled-cluster theory embedded in density functional theory. *The Journal of Chemical Physics* **2013**, *139*, 104106.

15. Jacob, C. R.; Neugebauer, J. Subsystem density-functional theory. *WIREs Computational Molecular Science* **2014**, *4*, 325–362.

16. Barcza, B.; Szirmai, A. B.; Tajti, A.; Stanton, J. F.; Szalay, P. G. Benchmarking Aspects of Ab Initio Fragment Models for Accurate Excimer Potential Energy Surfaces. *Journal of Chemical Theory and Computation* **2023**, *19*, 3580–3600.

17. Pipek, J.; Mezey, P. A Fast Intrinsic Localization Procedure Applicable For Abinitio And Semiempirical Linear Combination Of Atomic Orbital Wave-Functions. *J. Chem. Phys.* **1989**, *90*, 4916–4926.

18. Knizia, G. Intrinsic Atomic Orbitals: An Unbiased Bridge between Quantum Theory and Chemical Concepts. *Journal of Chemical Theory and Computation* **2013**, *9*, 4834–4843.

19. Claudino, D.; Mayhall, N. J. Automatic Partition of Orbital Spaces Based on Singular Value Decomposition in the Context of Embedding Theories. *Journal of Chemical Theory and Computation* **2019**, *15*, 1053–1064.

20. Khait, Y. G.; Hoffmann, M. R. In *Annual Reports in Computational Chemistry*; Wheeler, R. A., Ed.; Annual Reports in Computational Chemistry; Elsevier, 2012; Vol. 8; pp 53–70.

21. Claudino, D.; Mayhall, N. J. Simple and Efficient Truncation of Virtual Spaces in Embedded Wave Functions via Concentric Localization. *The Journal Chemical Theory and Computations* **2019**, *15*, 6085 – 6096.

22. Bennie, S. J.; Stella, M.; Miller, I., Thomas F.; Manby, F. R. Accelerating wavefunction in density-functional-theory embedding by truncating the active basis set. *The Journal of Chemical Physics* **2015**, *143*, 024105.

23. Senjean, B.; Sen, S.; Repisky, M.; Knizia, G.; Visscher, L. Generalization of Intrinsic Orbitals to Kramers-Paired Quaternion Spinors, Molecular Fragments, and Valence Virtual Spinors. *Journal of Chemical Theory and Computation* **2021**, *17*, 1337–1354.

24. Sen, S.; Senjean, B.; Visscher, L. Characterization of excited states in time-dependent density functional theory using localized molecular orbitals. *The Journal of Chemical Physics* **2023**, *158*, 054115.

25. Barcza, B.; Szirmai, Á. B.; Szántó, K. J.; Tajti, A.; Szalay, P. G. Comparison of approximate intermolecular potentials for ab initio fragment calculations on medium sized N-heterocycles. *Journal of Computational Chemistry* **2022**, *43*, 1079–1093.

26. Boughton, J. W.; Pulay, P. Comparison of the Boys and Pipek–Mezey localizations in the local correlation approach and automatic virtual basis selection. *Journal Of Computational Chemistry* **1993**, *14*, 736 – 740.

27. Kállay, M.; Nagy, P. R.; Mester, D.; Gyevi-Nagy, L.; Csóka, J.; Szabó, P. B.; Rolik, Z.; Samu, G.; Csontos, J.; Hégely, B.; Ganyecz, Á.; Ladjánszki, I.; Szegedy, L.; Ladóczki, B.;

Petrov, K.; Farkas, M.; Mezei, P. D.; Horváth, R. A. MRCC, a quantum chemical program suite. See https://www.mrcc.hu/, Accessed December 1, 2023.

28. Kállay, M.; Nagy, P. R.; Mester, D.; Rolik, Z.; Samu, G.; Csontos, J.; Csóka, J.; Szabó, P. B.; Gyevi-Nagy, L.; Hégely, B.; Ladjánszki, I.; Szegedy, L.; Ladóczki, B.; Petrov, K.; Farkas, M.; Mezei, P. D.; Ganyecz, A. The MRCC program system: Accurate quantum chemistry from water to proteins. *The Journal of Chemical Physics* **2020**, *152*, 074107.

29. Bartlett, R. J.; Purvis III, G. D. Molecular Applications of Coupled Cluster and Many-Body Perturbation Methods. *Phys. Scr.* **1980**, *21*, 255–265.

30. Stanton, J. F.; Bartlett, R. J. The Equation of Motion Coupled-Cluster Method - A Systematic Biorthogonal Approach to Molecular-Excitation Energies, Transition-Probabilities, and Excited-State Properties. *J. Chem. Phys.* **1993**, *98*, 7029–7039.

31. Comeau, D. C.; Bartlett, R. J. The Equation-of-Motion Coupled-Cluster Method - Applications to Open-Shell and Closed-Shell Reference States. *Chem. Phys. Lett.* **1993**, *207*, 414–423.

32. Perdew, J. P.; Burke, K.; Ernzerhof, M. Generalized Gradient Approximation Made Simple. *Phys. Rev. Lett.* **1996**, *77*, 3865–3868.

33. Grimme, S.; Antony, J.; Ehrlich, S.; Krieg, H. A consistent and accurate ab initio parametrization of density functional dispersion correction (DFT-D) for the 94 elements H-Pu. *The Journal of Chemical Physics* **2010**, *132*, 154104.

34. Shahbaz, M.; Szalewicz, K. Do Semilocal Density-Functional Approximations Recover Dispersion Energies at Small Intermonomer Separations? *Physical Review Letters* **2018**, *121*, 113402.